

# Direct Observations of Wave Induced Sediment Flux and Turbulent Velocities in a Wave Flume

Len Zedel<sup>1</sup> and Alex Hay<sup>2</sup>

1. Memorial University of Newfoundland, St. John's, NF, A1B 3X7

2. Dalhousie University, Halifax, NS, B3H 4J1

## 1. INTRODUCTION

Knowledge of the vertical distribution of suspended sediment is required to model the transport of sediment due to wave action. In order to better understand the sediment suspension process and the contributions of turbulent fluctuations in particular, it is important that collocated measurements of suspended particle concentration and velocity be made. Such observations are lacking and are particularly needed for comparison with model predictions.

We present acoustic measurements of vertical velocity and suspended sediment concentration using a coherent Doppler sonar (Zedel et al. 1996). The 1.7 MHz, Dopbeam system was configured to provide velocity profiles with 1.4 cm range resolution and a  $0.5 \text{ cm s}^{-1}$  vertical velocity accuracy at a rate of 30 profiles per second. Concentration measurements are acquired at the same time and location through calibration of the acoustic backscatter levels to absolute concentrations for the sediment samples used. The Dopbeam system has been calibrated using a sediment laden turbulent jet as described by (Hay 1991).

The measurements were made in the Wave Research Flume at the National Research Council (Ottawa), Canada. This facility has a length of 100 m, a width of 2.0 m and was filled to a water depth of 1.8 m. A 10 cm thick layer of  $150 \mu\text{m}$  (sorted) sand was deposited through a 20 m long test section. Observations were made with regular and irregular waves with nominal heights of 20 to 70 cm.

## 2. VERTICAL FLUX

The vertical flux of sediment can be expressed as;

$$\vec{F} = \langle \bar{w}\bar{c} + \tilde{w}\tilde{c} + w'c' \rangle \quad (1)$$

where  $w$  is the vertical component of velocity,  $c$  is the concentration, the tilde and prime refer to wave and turbulent components respectively,  $\langle \rangle$  indicates a time average. The three terms on the right hand side of Equation (1) represent mean, wave induced, and turbulent vertical flux respectively: each of these terms are evaluated from the amplitude and Doppler shift of the backscattered signal as a function of height above the bed. Wave components were isolated by selectively averaging data according to the wave phase, the turbulent components were then determined as the residual after mean and wave components were removed. We find that the sum of these flux terms is approximately balanced as is shown by

the example in Fig. 1. The averaged mean flux is downward (settling) with the wave and turbulent flux being in an upward direction. The wave component of flux is relatively small and thus an approximate balance exists between the turbulent upward flux and the mean downward settling flux.

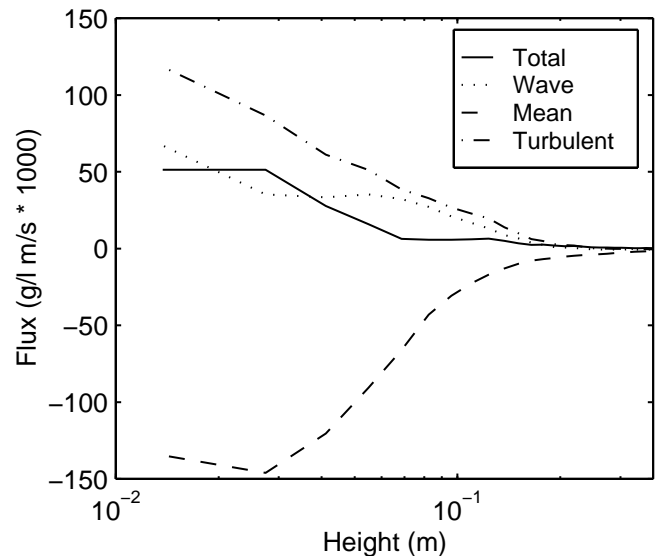


**Figure 1: Profiles of mean, wave, turbulent and total sediment flux. Profiles are based on a 6 minute data sample under regular, 3.5 s period waves of 60 cm height**

## 3. TURBULENCE INTENSITY

The energy driving sediment upward from the bottom is derived from turbulent fluid motions. This energy can be parameterised in terms of the friction velocity  $u_*$ . We have estimated the value of  $u_*$  from the characteristics of the suspended sediment concentration profiles following the approach used by Sheng and Hay (1995). Table 1 compares the values of  $u_*$  derived from this technique ( $u_*(\text{sediment})$ ) in Table 1) with parameterisations based on the waves and grain roughness (Nielson 1992) ( $u_*$  in Table 1).

An independent indicator of the turbulence characteristics of the boundary layer is provided by profiles of  $\langle w'_{rms} \rangle$ : example profiles are shown in Fig. 2. Nielsen (1992 p. 72) reports that peak values of  $\langle w'_{rms} \rangle = 0.5u_*$  occurring at a height approximately

equal to the top of the roughness elements. Similar relations are also seen in unidirectional boundary layer flow (Tennekes and Lumley 1972 p. 162). The peak values of  $\langle w'_{rms} \rangle$  in the present observations are very close to the parametric estimates of friction velocity as well as those based on concentration profiles (see  $w'_{max}$  in Table 1).

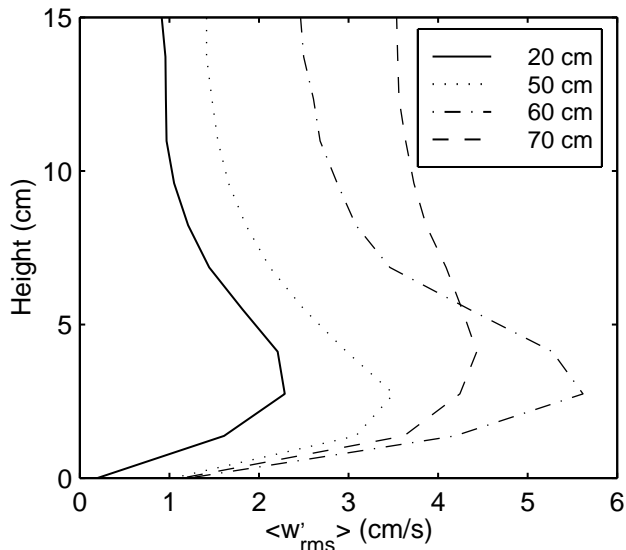


**Figure 2:** Profiles of  $\langle w'_{rms} \rangle$  as observed under 3.5 s period waves of height 20, 50, 60 and 70 cm.

**Table 1:** Summary of trials under 3.5 s period waves with heights indicated as H;  $u_*$  is the friction velocity computed from parameterisations of wave height,  $u_*(\text{sediment})$  is based on the near bottom profile of suspended sediment (Sheng and Hay, 1995),  $w'_{max}$  refers to the maximum observed variance in vertical velocity observations. Bedforms are indicated by  $R_l$ ,  $R_s$ ,  $X$ , and  $F$  for long crested, short crested, cross ripples, and flat bed respectively.

H cm	Bed Form	$u_*$ $\text{cm s}^{-1}$	$u_*(\text{sediment})$ $\text{cm s}^{-1}$	$w'_{max}$ $\text{cm s}^{-1}$
20	$R_l$	1.5	2.2	2.3
30	$R_s$	2.3	2.5	2.5
40	$R_s$	3.1	3.2	2.9
50	$X$	3.4	3.9	3.5
60	$X$	4.2	7.0	5.6
70	$F$	4.9	5.0	4.4

An important aspect of the data summarised in Table 1 is the apparent response to changing bedforms. In particular, the decrease in the observed indicators of friction velocity ( $u_*(\text{sediment})$ , and  $w'_{max}$  in Table 1), that occurs between 60 and 70 cm wave heights coincides with the disappearance of small

scale bedforms. The associated change in roughness is not accounted for in the parametric estimate of friction velocity but it is clearly important to regulating the turbulent contribution to sediment transport.

#### 4. CONCLUSIONS

Through the use of combined Doppler sonar and acoustic backscatter measurements it has been possible to make simultaneous estimates of particle velocity and concentration. This combination of measurements allows for direct observation of particle flux. Phase averaging under regular waves (possible in the tow tank test facility) allows the discrimination of both turbulent and wave components of flux  $w'c' + \tilde{w}\tilde{c}$  in addition to the mean (downward) flux.

The assumption of a balance between the wave and turbulence induced upward flux of sediment with the mean downward flux is fundamental to most models of vertical sediment transport (see for example Lee and Hanes 1996). We have demonstrated that such a balance does exist in the present data. Previous estimates of the downward flux term have been made from independent measurements of particle descent rate and concentration: a common assumption is that the particle descent rate is given by the free descent rate of the particles (Sheng and Hay, 1995). This assumption appears to hold for most of the water column but breaks down within 5 cm of the bottom in the present observations.

The turbulent velocity represented by  $\langle w'_{rms} \rangle$  reaches a peak a small distance above the bed (within 5 cm in the present observations). At heights above the peak value,  $\langle w'_{rms} \rangle$  decays as  $1/\text{height}$ , consistent with Sleath 1991. The (near bottom) peak values of  $\langle w'_{rms} \rangle$  are equal to the friction velocity characteristic of the bottom boundary layer (as estimated parametrically and from the concentration profile). We conclude that the direct observation of  $\langle w'_{rms} \rangle$  possible with the coherent Doppler system is an effective means of estimating friction velocity.

#### 5. REFERENCES

- Hay, A.E., 1991. J. Acoust. Soc. Am., 90, 2055-2074.
- Lee, T.H. and D.M. Hanes, 1996. J. Geophys. Res., 101, 3561-3572.
- Nielsen, P., 1992: Coastal bottom boundary layers and sediment transport. World Scientific, Singapore, 324 pp.
- Sheng, J., and A.E. Hay, 1995. Cont. Shelf Res., 15, 2/3, 129-147.
- Sleath, J.F.A., 1991. J. Geophys. Res. 96, C8, 15237-15244.
- Tennekes, H. and J.L. Lumley, 1972: A first course in turbulence. MIT Press, Cambridge, 300 pp.
- Zedel, L., A.E. Hay, R. Cabrera, and A. Lohrmann, 1996. IEEE Journal of Oceanic Technology, 21, 290-297.

# Figures